

Supporting information

**Chemical operations on a living single cell by open microfluidics
for wound repair studies and organelle transport analysis**

*Sifeng Mao,^a Qiang Zhang,^a Wu Liu,^a Qiushi Huang,^a Mashooq Khan,^a Wanling Zhang,^a Caihou Lin,^b Katsumi Uchiyama,^c and Jin-Ming Lin^{*a}*

^a Department of Chemistry, Beijing Key Laboratory of Microanalytical Methods and Instrumentation, MOE Laboratory of Bioorganic Phosphorus Chemistry & Chemical Biology, Tsinghua University, Beijing 100084, China. E-mail: jmlin@mail.tsinghua.edu.cn

^b Department of Neurosurgery, Fujian Medical University Union Hospital, Fuzhou, Fujian 350001, China

^c Department of Applied Chemistry, Graduate School of Urban Environmental Sciences Tokyo Metropolitan University, Minamiohsawa, Hachioji, Tokyo 192-0397, Japan.

**Corresponding author. Email: jmlin@mail.tsinghua.edu.cn*

Methods

Design and fabrication of the fluid cell knife (Fluid CK). The Fluid CK were fabricated by a capillary stretching technique with a heat puller (PB-7, NARISHIGE, Tokyo, Japan). Simply, four identical glass tubes (800 μm i.d., 1300 μm o.d.) were gathered together by using heat shrink tubes. Then, they were positioned on the heat puller. They were pulled to give two devices (upper, lower sides) under high temperature. Finally, we polished the device on a sand paper to get a Fluid CK with smooth bottom surface. The manufacture process was described in Figure S1.

Operation system. The operation system contained a positioning system, an XY motion control system and a flow injection and aspiration system. In the positioning system, an XYZ stage (Sigma KOKI Co., Ltd.) served as the device holder for positioning the Fluid CK to desirable point and gap between the bottom surface of the Fluid CK and the sample surface. In the XY motion control system, cell samples were placed on the XY stage of an inverted microscope (Leica DMI 4000 B, Wetzlar, Germany) or a confocal microscope (IX83, Olympus, Japan). In the flow injection and aspiration system, four apertures of the Fluid CK were connection to four gas tight syringes (Hamilton, Graubunden, Switzerland) by PEEK tube (GL Science, Tokyo, Japan). The two syringes for flow injection were driven by a syringe pump (Hamilton, Pennsylvania, USA), and the other two were driven by another syringe pump.

In all of the experiments, the Fluid CK was maintained at its position while the position of cell samples were controlled by the XY stage of the microscope. A petri dish (Corning, New York, USA) with cell sample, filled with cell culture medium, was placed on the XY stage of a microscope. Then, the Fluid CK was immersed in the cell culture medium and placed perpendicular to the surface of petri dish with a certain gap. The Fluid CK was fixed on an XYZ stage that functioned as a positioner. The XYZ stage contains three dividing rulers to monitor distance change in X, Y or Z directions. The resolution of the rulers on our XYZ stage was 5 μm . To well address the gap in experiments, we moved down the Fluid CK by controlling the XYZ stage to make it just to touch the substrate where gap was “Zero”. Then, we raised the Fluid CK in Z

direction by using the positioner with a desired distance (50 μm), resulting in a gap of 50 μm between bottom surface of the Fluid CK and substrate.

Finite element analysis. Comsol Multiphysics 5.3b (Comsol) was used to carry out 3D simulations on a six-core, 64-bit computer (Dell) with 32 GB of RAM. The geometry of the Fluid CK was set as same as that in the experiment. Four circular apertures (i.d. 120 μm) were included in the geometry. The center of each formed a square shape with a side of 500 μm . The gap between the bottom surface of the Fluid CK and the sample surface was set as 50 μm . Injection flow rate was 1 $\mu\text{L}/\text{min}$ and the aspiration flow rate was 10 $\mu\text{L}/\text{min}$. The injection solution was assumed to be water with a density of 999.7 kg/m^3 and a viscosity of 0.001 $\text{Pa}\cdot\text{s}$. The simulations were run under steady-state conditions with the flow boundary conditions at the edges of the microfluidic chip probe perimeter sides set as open boundaries (equal to atmospheric pressure).

Characterization of the Fluid CK. The shape and the bottom surface of the Fluid CK were examined by a scanning electron microscope (SEM, 5100N, Hitachi High Technologies, Japan).

Cell culture and sample preparation. U87 cells, Caco-2 cells, HepG2 cell, MCF-7 and HUVEC cells were purchased from Cancer Institute & Hospital of the Chinese Academy of Medical Science (Beijing, China). All cells were cultured in a humidified atmosphere of 95% air and 5% CO_2 at 37 $^\circ\text{C}$. U87 cells were maintained in minimal essential medium (MEM, Corning, USA) with Earle's Salts and L-glutamine supplemented with 10% fetal bovine serum (FBS, Corning, USA), nonessential amino acids, 100 units/mL penicillin, and 100 units/mL streptomycin. Caco-2 cells were maintained in RPMI-1640 (Corning, USA) with Earle's Salts and L-glutamine supplemented with 10% FBS, nonessential amino acids, 100 units/mL penicillin, and 100 units/mL streptomycin. HepG2, MCF-7 and HUVEC cells were maintained in Dulbecco's modified Eagle's minimal essential medium (DMEM, Corning, USA) with high glucose supplemented with 10% FBS, nonessential amino acids, 100 units/mL penicillin, and 100 units/mL streptomycin. All types of cells were maintained in Petri dishes for 2–3 days prior to commencing the experiments. All the experiments were

carried out when the cells were in the exponential growth phase. Cells were detached from the Petri dishes with 0.25% trypsin, resuspended in corresponding cell-culture medium, counted with a hemocytometer and moved to Petri dishes at a final density of $\sim 1 \times 10^4$ cells/cm². Cells were maintained in the Petri dishes for at least 12 h for cell adherence prior to cell detachment experiments.

Investigation of the interface between two injected flows. Solution containing 1 $\mu\text{g/ml}$ fluorescein for visualization, was used to verify the zone of one injected solution and the interface between the two adjacent solutions. In all the experiments, gap was kept as 50 μm . Firstly, we examined different flow ratio R_a/R_i while keeping a constant injection flow rate (1 $\mu\text{L/min}$). The ratio was optimized to be 10. Then, different flow rates were applied under a constant ratio ($R_a/R_i = 10$). The position deviation of the interface were evaluated.

Precise cell cutting and wound repair. RIPA non-denatured tissue lysis buffer (R0030, Solarbio, China) was used in cell cutting experiments for lysing portion of cell. The lysis buffer was one injected solution and cell culture medium was the other one. A stable planar interface between the lysis buffer and the culture medium appeared. The target single-cell was firstly positioned in the culture medium zone, and then moved towards the interface to make part of the cell reach the lysis buffer zone. The portion of cell immersing in the lysis buffer was cut off rapidly. The lysis process could be observed in real time. Five different types of cells (U87, HUVEC, Caco-2, MCF-7 and HepG2 cells) were treated to demonstrate the feasibility of the device for precise cell cutting. After partial lysis, the probe was removed and the cell was cultured for a period of time in the incubator. Live/Dead Kit containing 4.5 $\mu\text{mol/L}$ Propidium Iodide (PI) and 2 $\mu\text{mol/L}$ Calcein-AM (diluted in MEM basal culture medium) was used to stained the cell for 15 min after incubation. Then, the bright-field image and fluorescent images were recorded using the microscope.

Subcellular molecule infusion to a single-cell. MitoTracker Deep Red FM (0.5 μM , Yeasen, China) and MitoTracker Green FM (1 μM , Yeasen, China) were prepared in phosphate buffer (PBS, 0.01 M, pH = 7.4). The two dye-solutions were injected. Single

U87 cell was positioned at the interface for subcellular molecule infusion. Portion of the cell was treated with MitoTracker Deep Red FM, while the other portion was treated with MitoTracker Green FM. The mitochondrion in different portions would be stained with the two different fluorescent dyes after 3 min. In the same manner, ER-Tracker Red (1 μM) and ER-Tracker Green (1 μM) were prepared in PBS solution. They two performed as the two injected solutions for partial staining endoplasmic reticulum in cell after 5 min. In all those experiments, data was recorded by a confocal microscope (IX83, Olympus, Japan). The working conditions of the Fluid CK were: $R_i = 1 \mu\text{L min}^{-1}$, $R_a = 10 \mu\text{L min}^{-1}$, $\text{gap} = 50 \mu\text{m}$.

Monitoring of organelle transport in a single-cell. MitoTracker Deep Red FM solution was used as a model to monitor the transport of mitochondrion. MitoTracker Red solution was injected and flowed out from the lower left aperture and cell culture medium was injected and flowed out from the upper right aperture. A planar interface formed between the two injections under the effect of high aspiration. Single U87 cell was moved to and positioned at the interface, thus its lower left portion was immersed in MitoTracker solution while upper right portion in cell culture medium. After 3 min, the Fluid CK was moved away from and the transport of the stained mitochondrion was recorded then by a confocal microscope (IX83, Olympus, Japan). For convenience, the time was set as Zero when the record started. Data was recorded. The working conditions of the Fluid CK were: $R_i = 1 \mu\text{L min}^{-1}$, $R_a = 10 \mu\text{L min}^{-1}$, $\text{gap} = 50 \mu\text{m}$. The recorded images were analyzed using Image-Pro plus software (Media Cybernetics Inc., Bethesda, MD, USA).

Supplementary Figures

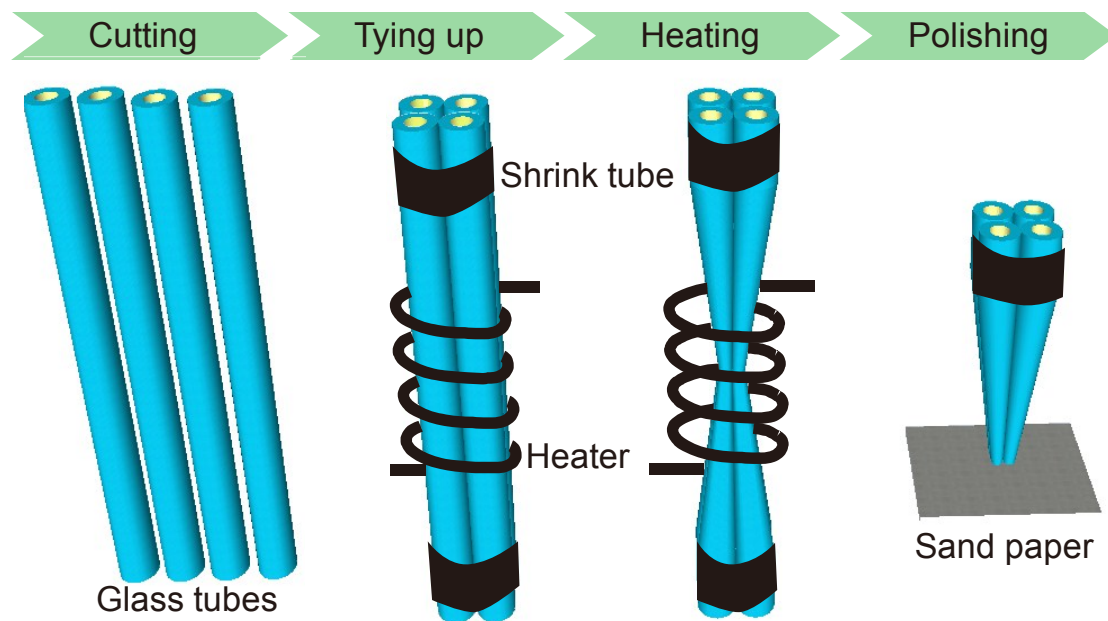


Figure S1. The manufacture process of the Fluid CK.

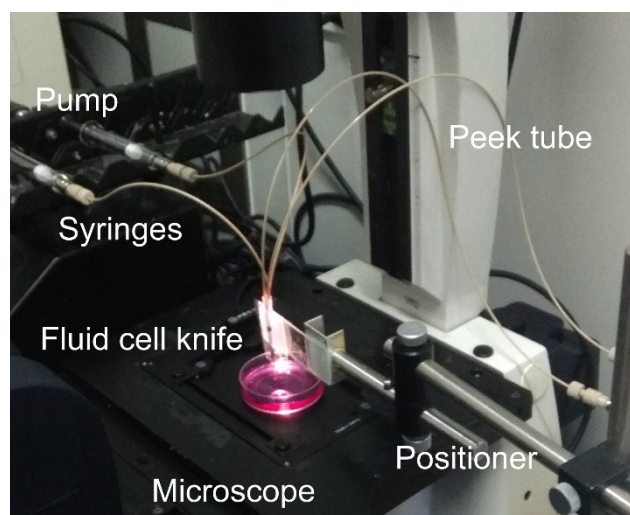


Figure S2. Experimental setup of the operation system.

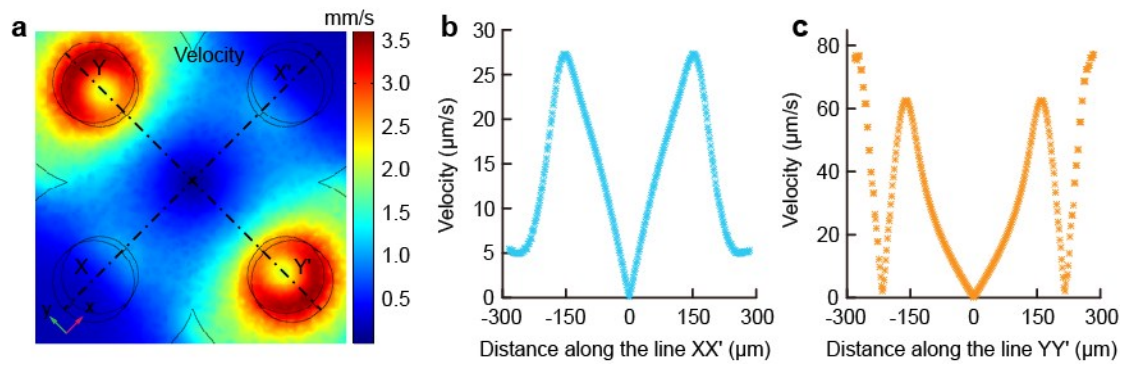


Figure S3. Calculated velocity in the simulation. a) Velocity distributions of the diffusive species at the substrate. b) Velocity profile of the diffusive species at the substrate along the line XX' connecting the two injection apertures. c) Velocity profile of the diffusive species at the substrate along the line YY' connecting the two aspiration apertures.

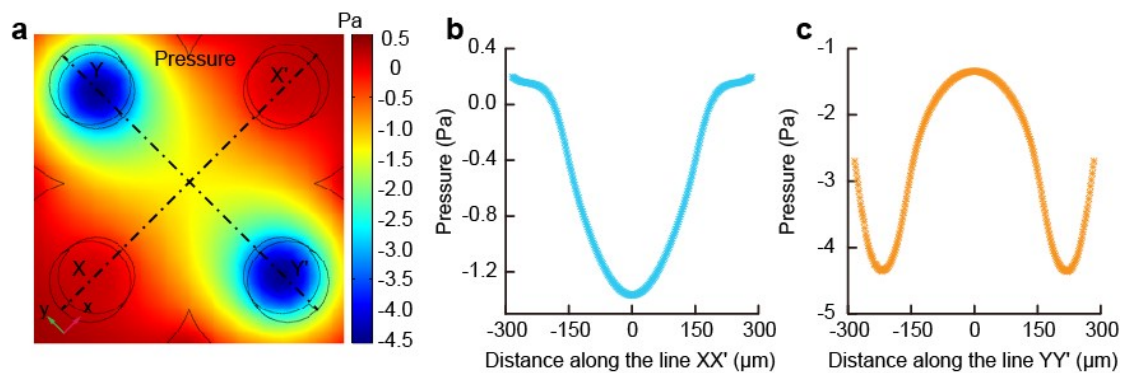


Figure S4. Calculated pressure in the simulation. a) Pressure distributions of the diffusive species at the substrate. b) Pressure profile of the diffusive species at the substrate along the line XX' connecting the two injection apertures. c) Pressure profile of the diffusive species at the substrate along the line YY' connecting the two aspiration apertures.

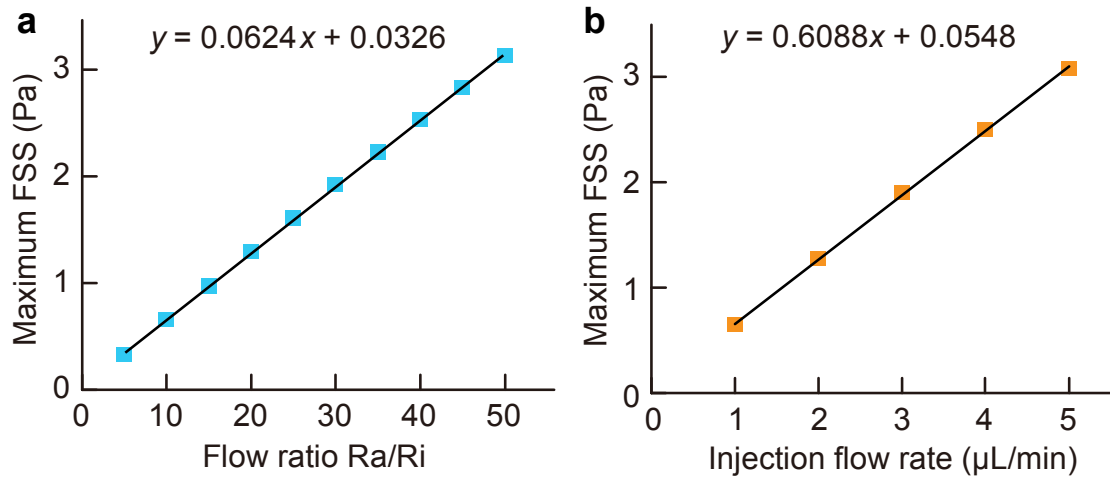


Figure S5. Maximum fluid shear stress under different conditions in the simulation. a) Maximum fluid shear stress under different flow ratio Ra/Ri. b) Maximum fluid shear stress under different injection flow rate.

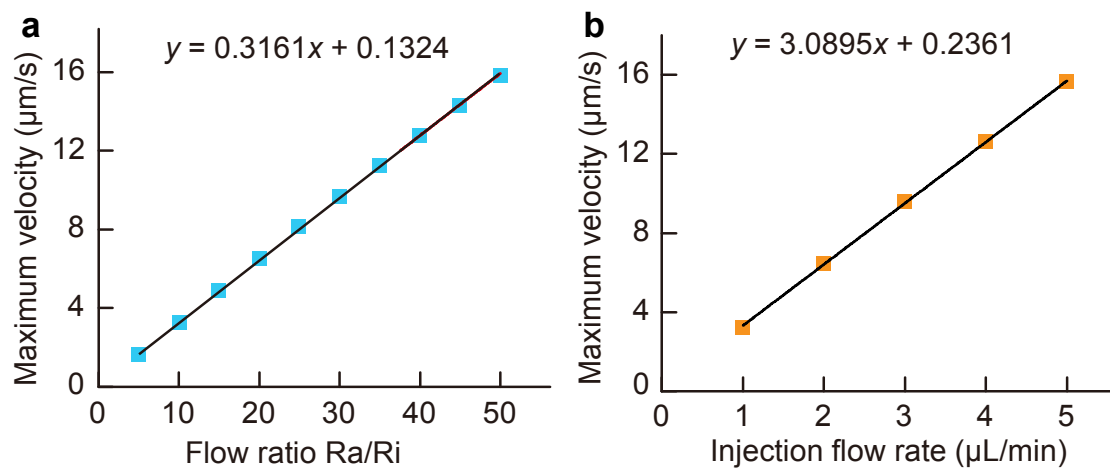


Figure S6. Maximum line velocity under different conditions in the simulation. a) Maximum velocity under different flow ratio Ra/Ri. b) Maximum velocity under different injection flow rate.

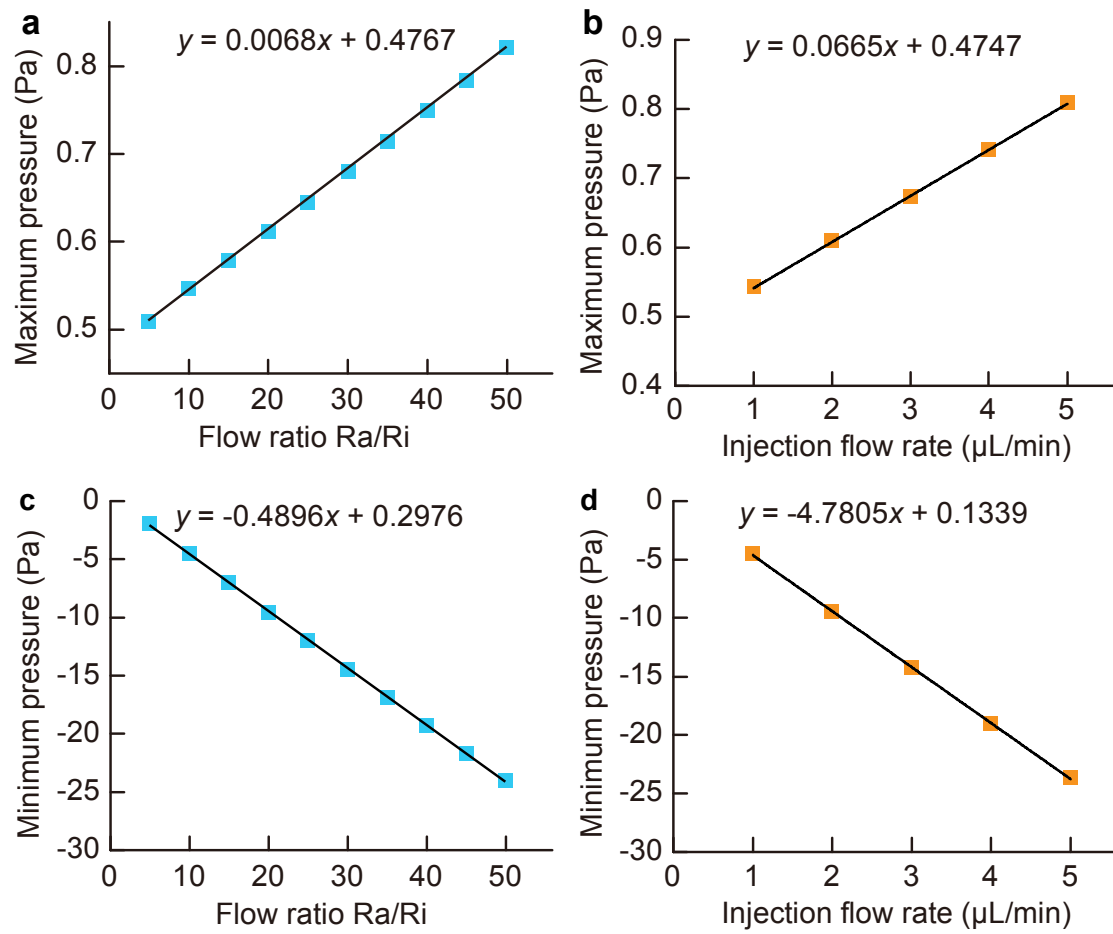


Figure S7. Maximum velocity and minimum velocity under different conditions in the simulation. a) Maximum pressure under different flow ratio Ra/Ri. b) Maximum pressure under different injection flow rate. c) Minimum pressure under different flow ratio Ra/Ri. d) Minimum pressure under different injection flow rate.

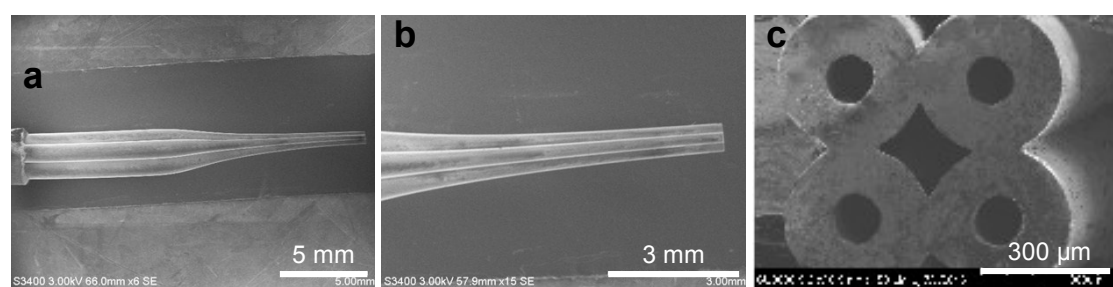


Figure S8. SEM image of the Fluid CK. a) SEM image of the Fluid CK. b) SEM of the tip of the Fluid CK. c) SEM image of the bottom surface of the tip.

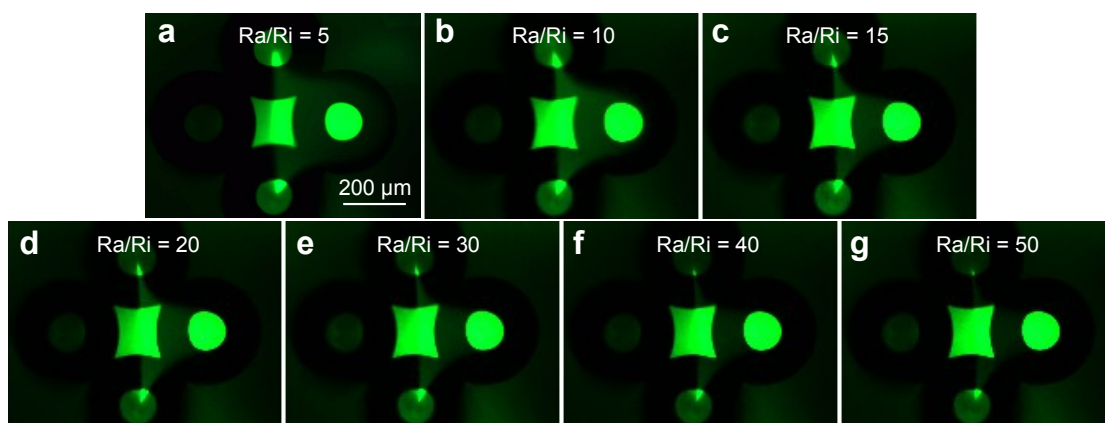


Figure S9. Fluorescent image of the microjet underneath the Fluid CK in the experimental results under different flow ratios a) 5, b) 10, c) 15, d) 20, e) 30, f) 40, g) 50. The injection flow rate was constant ($Ri = 1 \mu\text{L}/\text{min}$).

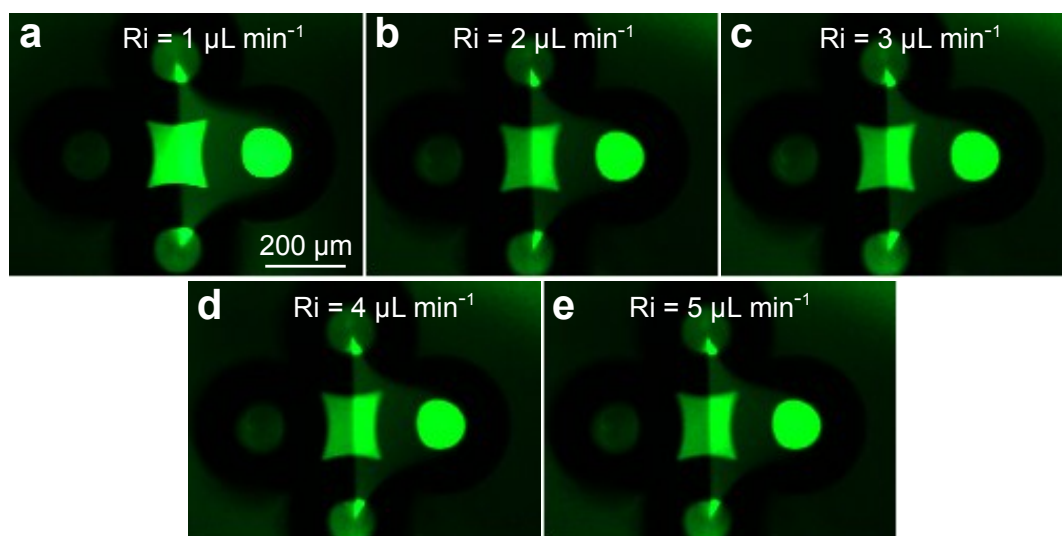


Figure S10. Fluorescent image of the microjet underneath the Fluid CK in the experimental results under different injection flow rates a) $1 \mu\text{L}/\text{min}$, b) $2 \mu\text{L}/\text{min}$, c) $3 \mu\text{L}/\text{min}$, d) $4 \mu\text{L}/\text{min}$, e) $5 \mu\text{L}/\text{min}$. The flow ratio Ra/Ri was constant (equal to 10).

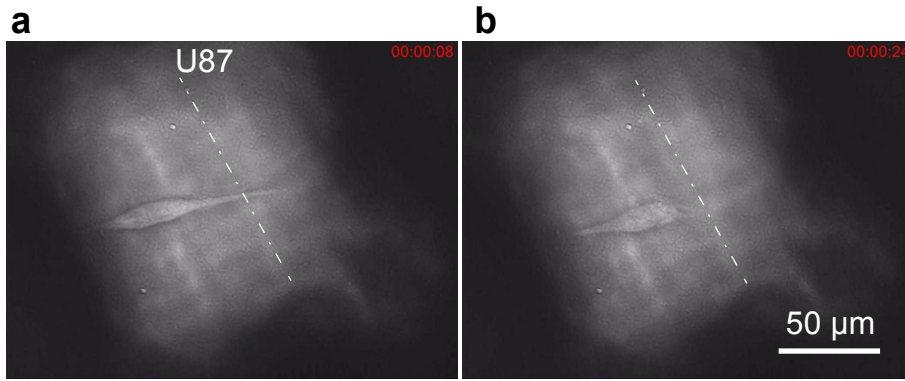


Figure S11. Subcellular cutting of U87 cell. (a) Bright-field image of cell before cutting. (b) Bright-field image of cell after cutting.

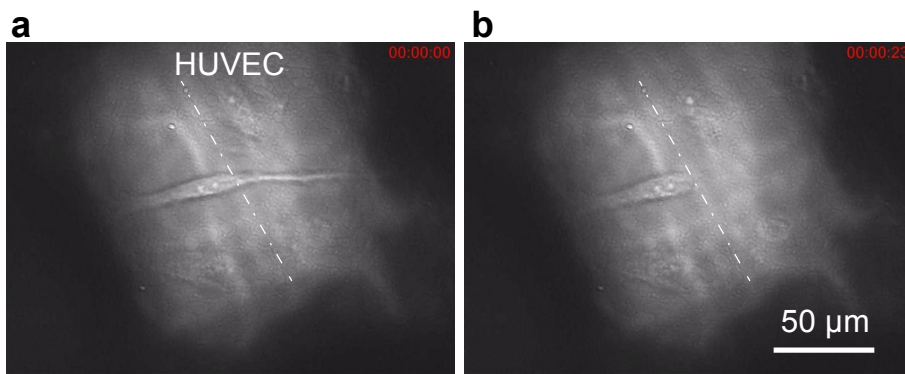


Figure S12. Subcellular cutting of HUVEC cell. (a) Bright-field image of cell before cutting. (b) Bright-field image of cell after cutting.

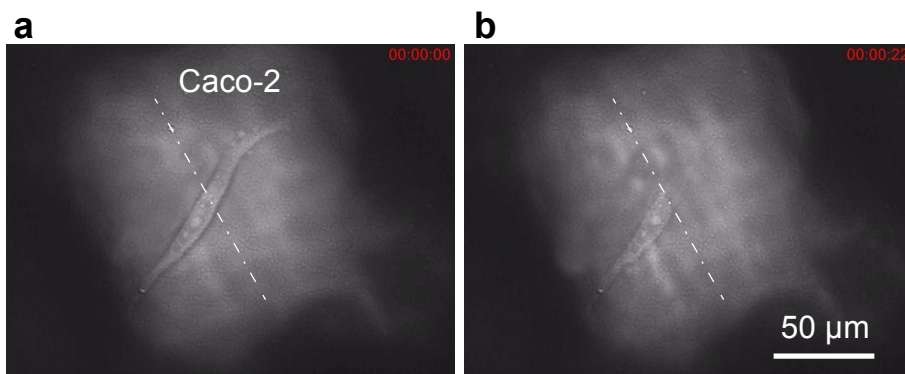


Figure S13. Subcellular cutting of Caco-2 cell. (a) Bright-field image of cell before cutting. (b) Bright-field image of cell after cutting.

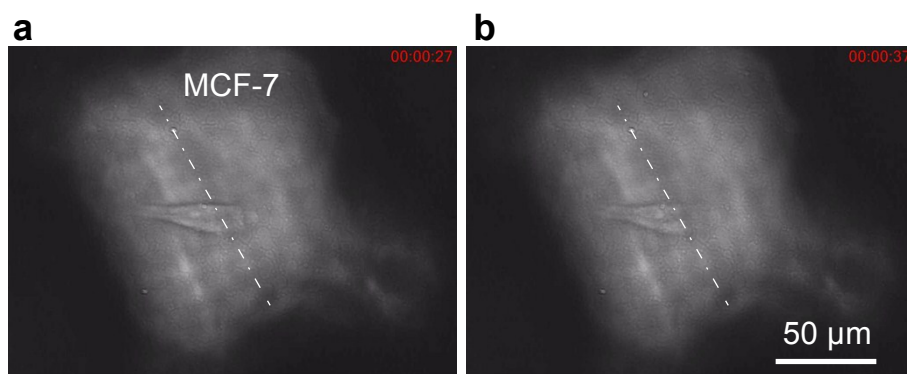


Figure S14. Subcellular cutting of MCF-7 cell. (a) Bright-field image of cell before cutting. (b) Bright-field image of cell after cutting.

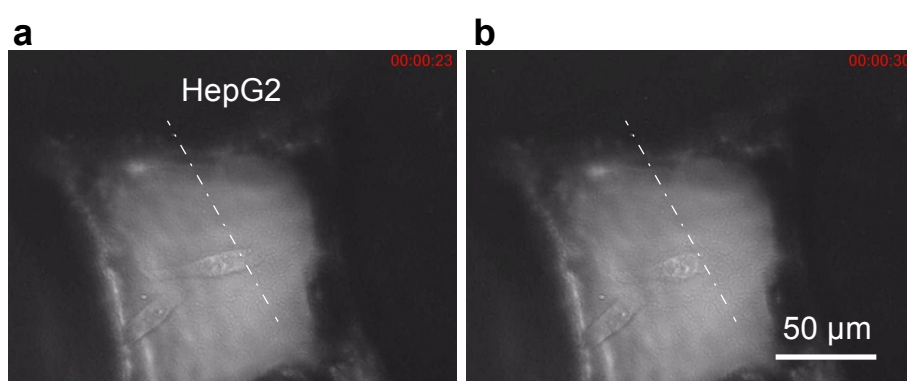


Figure S15. Subcellular cutting of HepG2 cell. (a) Bright-field image of cell before cutting. (b) Bright-field image of cell after cutting.

Supplementary movies:

Supplementary movie S1. Fluid cell knife